JCAMECH

Vol. 49, No. 1, June 2018, pp 1-8
DOI: 10.22059/jcamech.2018.255680.264

On The Effect of Nanofluid Flow and Heat Transfer with Injection through an Expanding or Contracting Porous Channel

Olofinkua Joseph Olawale[*]

Department of Mechanical Engineering, University of Lagos, Akoka- Yaba, Lagos, Nigeria.

ARTICLE INFO

Article history:
Received: 14 Apr. 2018
Accepted: 17 May. 2018

Keywords:
Heat transfer
Nanofluid
Porous channel
Magnetic Field
Regular perturbation method

ABSTRACT

The studies of the behavior of fluid on the nano-level has shown to be an important means of influencing the characteristic of fluid must especially in the area of thermal conductivity. Giving relevance in numerous fields such as biomedicine, manufacturing, fuel cells and soon on. This article considers flow and heat transfer of viscous fluid conveying Gold nanoparticles through expanding or contracting porous channel with injection. The nanofluid is described by the high order coupled nonlinear equations of the fourth order which is analyzed utilizing the regular perturbation method whose analytical solutions is adopted in describing the effect of various thermal-fluidic parameters such as Reynolds number and temperature power index. Where results reveals that increasing Reynolds causes an increasing velocity distribution while increasing temperature power index demonstrates decreasing temperature effect. Also comparison of obtained analytical solution against numerical solution shows satisfactory agreement. Study provides good advancement to applications such as fluid transport, power plant operations and manufacturing amongst others.

1. Introduction

Study of fluid flow through porous channels has generated interest amongst researchers over the years owing to their ever increasing application in science and engineering. Finding vast importance in industrial fields such as reservoir engineering, flow through porous industrial materials, heat exchange between fluid beds, ceramic processing, polymer solution, food technology, environmental protection, power plant operations, manufacturing, transportation and oil recovery amongst others. In recent past, efforts to study flow and heat transfer have been extensive utilizing the numerous techniques available to analysis and understand its effects. Numerical methods was adopted by Pourmehran et al. [1] in optimizing nanofluid flow in saturated porous medium while Tang and Jing [2] investigated sinusoidal wavy cavity effect of heat transfer under natural convection with phase deviation. High accuracy spherical motion particle was presented by Hatami et al. [3] in coquette fluid film flow. Hatami and Song [4] optimized circular wavy cavity nanofluid flow under natural convection. Ghasemi et al. [5] utilized least square methods of weighted residuals to analyze electro-hydrodynamic effect of fluid flowing through a circular conduit, shortly after Ghasemi et al. [6] studied blood flow through porous arteries under the influence of magnetic force field with nanoparticles. Multi step differential transform method was applied by Hatami and Ganji [7] to analyze spherical particle motion of a rotating parabola. While Hatami and Jing [8] optimized lid driven T-shaped porous cavity in the bid to improve mixed convective heat transfer. Non-Newtonian fluid flow under natural convection through vertical parallel plates was investigated by Karger and Akbarzade [9]. Fakour et al. [10] presented micropolar flow and heat transfer flowing in a channel with permeable walls. Nanoparticle migration around heated cylinder was studied by Hatami [11] considering wavy enclosure wavy. In the bid to improve the thermal conductivity of viscous fluids such as water, oils, grease, ethylene. Choi [12] presented a novel approach to improving thermal conductivity of incompressible fluid through the addition of nanometer sized particle into the base fluid, where it was observed that upon the addition of

[*] Corresponding author. Tel.:+234-703-032-7149;
e-mail: josepholofinkua@yahoo.com

metallic nanosized particle into base fluid thermal conductivity of fluid improves to about three times it present state . Farajpour et al [13] examined the stresses on microtubules (MTs) embedded in an elastic medium in a thermal environment using zinc oxide (ZnO). It was found that the applied electric voltage can be used as an effective controlling parameter for the vibration and buckling of MTs. Other research works as relates to nano fluids and heat transfer includes a study pulsed flow and heat transfer in water-Al_2O_3 nanofluids in a Y-Type intersection channel by Wu et al [14]. The effects of pulse frequency, pulse amplitude and nanoparticles concentration on the heat transfer are explored numerically at various Reynolds numbers. The results show that the application of the pulsed flow through variation in frequency, amplitude and nanoparticles concentration was seen to improve the heat transfer efficiency. Sun et al [15] investigated the application of nanofluids as heat carrier fluid in a geothermal exchanger studying the stability of nanofluids by numerically simulating nanoparticle sedimentation. The nanofluids were seen to enhance the conductive and convective heat transfer in the exchanger. Therefore improving the overall transport capability of fluids making them potentially useful in fields such as biomedicine, manufacturing, fuel cells, and hybrid power generators amongst other practical application. These have created renaissance amongst researchers in science and engineering to explore the useful potential of nanofluid [16-22].

Since higher order nonlinear equations which describes the flow and heat of the nanofluid requires the use of approximate analytical or numerical methods of solution to analyze the system of coupled equations, the regular pertubation method is selected as the favoured scheme adopted to generate solution. Other approximate analytical methods of solutions applied by researchers in study of the heat transfer include the Adomian Decomposition Method (ADM), Homotopy Analysis Method (HAM), Variational Parameter Method (VIM), Differential Transformation Method (DTM) and methods of weighted residuals [23-33]. Methods such as DTM, HAM and ADM however require the need to find an initial condition that will satisfy the boundary condition which theories have not been rigorously proven for all cases. Making it necessary to use computational tools resulting to higher computational cost to provide problem solutions. Since, the solutions reported for the other relatively sophisticated methods to nonlinear problems have good accuracy, but they are more complicated for applications than perturbation methods. Although, perturbation method is valid only for weakly nonlinear problems and the method has also limited success with more complex problems, perturbation methods often prove valuable in shedding light on the physics of problems. Hence, over the years, the relative simplicity and high accuracy especially in the limit of small parameter which the perturbation method affords has made it an interesting tool among the most frequently used approximate analytical methods [22-25].

Motivated by past research works, the regular pertubation method is used to analyze the unsteady flow and heat transfer of a viscous fluid conveying gold nanoparticles with injection through an expanding/contracting porous channel.

2. Model Development and Analytical Solution

The fluid in consideration is a viscous fluid conveying gold nanoparticles which flows unsteadily through a porous channel. The upper plate expands and contracts with time while the lower plate is stationary and is externally heated which is described in the physical model diagram Fig. 1. The heated wall is cooled by injecting cool fluid with uniform velocity v_w from the upper plate which expands and contract at time rate a(t). Both plates are however perpendicular to y-axis. Where u and v is the velocity component of x and y direction. According to this view fluid flow may be assumed to be stagnation flow. The model development is done by assuming a two component nanofluid mix, incompressible fluid flow since fluid is liquid, negligible radiation effect, nanoparticle and base fluid are in thermal equilibrium. Therefore owing to these condition Navier – Stokes equation can be presented as:

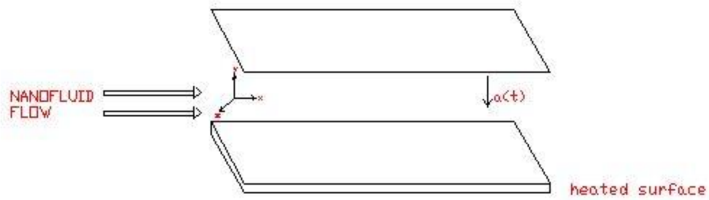

Figure 1. Physical Model of Problem.

$$\frac{\partial u}{\partial x}+\frac{\partial v}{\partial y}=0 \tag{1}$$

$$\rho_{nf}\left(\frac{\partial u}{\partial t}+u\frac{\partial u}{\partial x}+v\frac{\partial u}{\partial y}\right)=-\frac{\partial p^*}{\partial x}+\mu_{nf}\left(\frac{\partial^2 u}{\partial x^2}+\frac{\partial^2 u}{\partial y^2}\right) \tag{2}$$

$$\rho_{nf}\left(\frac{\partial v}{\partial t}+u\frac{\partial v}{\partial x}+v\frac{\partial T}{\partial y}\right)=-\frac{\partial p^*}{\partial y}+\mu_{nf}\left(\frac{\partial^2 v}{\partial x^2}+\frac{\partial^2 v}{\partial y^2}\right) \tag{3}$$

$$\frac{\partial T}{\partial t}+u\frac{\partial T}{\partial x}+v\frac{\partial T}{\partial y}=\frac{k_{nf}}{(\rho C_p)_{nf}}\left(\frac{\partial^2 T}{\partial x^2}-\frac{\partial^2 T}{\partial y^2}\right) \tag{4}$$

where the effective density ρ_{nf} , effective dynamic viscosity μ_{nf} , heat capacitance $\left(\rho C_p\right)_{nf}$ and thermal conductivity k_{nf} of the nanofluid are defined as follows [19]:

$$\rho_{nf}=(1-\phi)\rho_f+\phi\rho_s \tag{5}$$

$$\left(\rho C_p\right)_{nf}=(1-\phi)(\rho C_p)_f+\phi(\rho C_p)_s \tag{6}$$

$$\mu_{nf}=\frac{\mu_f}{(1-\phi)^{2.5}} \tag{7}$$

$$A_1=\frac{k_{nf}}{k_f}=\frac{k_s+2k_f-2\phi(k_f-k_s)}{k_s+2k_f-\phi(k_f-k_s)} \tag{8}$$

Table 1. Thermo Physical Properties of Nanofluid

	Density (Kg/m^3)	Specific heat capacity(J/kgK)	Thermal conductivity(W/mk)
Water	997.1	4179	0.613
Gold (Au)	19300	129	318

with appropriate boundary condition stated as

$$u=0 \quad v=-v_w=-aA \quad T(a)=T_0 \quad at\ y=a(t)$$
$$u=0 \quad v=0 \quad at\ y=0 \tag{9}$$

where $A=v_w/a$ is the measure of wall permeability and T_0 is the porous plate temperature which as the same temperature of the injected coolant.

$$\psi = \frac{vx}{a} F(\eta, t) \tag{10}$$

Upon substituting Eq. (10) into Eqs. (1)- (3), eliminating pressure term from momentum equation. The following expression is obtained:

$$\psi = \frac{v_f x}{a} F(\eta, t) \tag{11}$$

Introducing these parameters:

$$F_{\eta\eta\eta\eta} + \frac{A_1}{A_2}\alpha\left(\eta F_{\eta\eta\eta} + 3F_{\eta\eta}\right) - FF_{\eta\eta\eta}$$

$$-F_\eta F_{\eta\eta} - \frac{A_1}{A_2}\alpha^2 v_f^{-1} F_{\eta\eta t} = 0 \tag{12}$$

where the wall expansion ratio is defined by α which is negative for contraction and positive for expansion.

$$\alpha = \frac{a\dot{a}}{v_f} \tag{13}$$

Nanofluid constant parameters A_1 and A_2 are expressed as:

$$A_1 = \frac{\rho_{nf}}{\rho_f} \tag{14}$$

$$A_2 = \frac{\mu_{nf}}{\mu_f} \tag{15}$$

where relevant boundary condition is given as

$$F_\eta(0) = 0 \quad F(0) = 0 \quad F_\eta(1) = 0 \quad F(1) = \frac{A_1}{A_2} R \tag{16}$$

R is the Reynolds number, which is positive for injection and negative for suction. Since injection is considered, R is positive.

$$f = \frac{F}{R}, l = \frac{x}{a} \tag{17}$$

For constant expansion rate α .A similar solution can be described for both time and space which leads to $f_{\eta\eta t}=0$ which is obtained by specifying the initial value of the expansion ratio.

$$\alpha = \frac{a\dot{a}}{v_f} = \frac{a_0 \dot{a}_0}{v_f} = Cte \tag{18}$$

where α_0 and a_0 connote initial channel height and expansion ratio respectively. Upon integrating Eq.9 with respect to time, this is simply expressed as:

$$\frac{a}{a_0} = \frac{v_w(0)}{v_w(t)} = \sqrt{1 + 2v_f \alpha t a_0^{-2}} \tag{19}$$

Since A is the coefficient for injection which is a constant. Therefore $v_w=Aa$, which is an expression for velocity variation of injection. Based on the above, the velocity profile is presented as:

$$\frac{d^4 f}{d\eta^4} + \frac{A_1}{A_2}\left(\alpha\left(\eta \frac{d^3 f}{d\eta^3} + 3\frac{d^2 f}{d\eta^2}\right)\right.$$

$$\left. + R\left(f \frac{d^3 f}{d\eta^3} - \frac{df}{d\eta}\frac{d^2 f}{d\eta^2}\right)\right) = 0 \tag{20}$$

with appropriate boundary condition introduced as

$$f(0) = 0 \quad \frac{df}{d\eta}(0) = 0 \quad f(1) = 1 \quad \frac{df}{d\eta}(1) = 1 \tag{21}$$

Fluid temperature from the wall at distance η is described as

$$T = T_0 + \sum C_m (x / a)^m q_m \tag{22}$$

The stationery heated wall temperature is expressed as:

$$\frac{d^2 q_m}{d\eta^2} - \frac{A_3}{A_4}\Pr Rmq_m \frac{df}{d\eta} + \frac{A_3}{A_4}\Pr Rf \frac{dq_m}{d\eta}$$

$$+\frac{A_3}{A_4}\alpha \Pr m q_m + \frac{A_3}{A_4}\Pr \eta\alpha \frac{dq_m}{d\eta} \tag{23}$$

where R is the Reynolds number which measures the significance of inertia compared to viscous fluid effect, α is the expansion ratio which predict the influence of expansion or contraction on fluid transport and Pr is the Prandtl no which determines the effect of momentum diffusivity against thermal diffusivity on nanofluid flow

Relevant constant parameters of the nanofluid are stated as:

$$A_3 = \frac{\left(\rho C_p\right)_{nf}}{\left(\rho C_p\right)_f}, A_4 = \frac{k_{nf}}{k_f} \tag{24}$$

with appropriate boundary condition expressed as

$$q_m(0) = 1, q_m(1) = 0 \tag{25}$$

Since single value for heat transfer coefficient cannot be obtained along the heated wall if wall temperature follows polynomial variation. Unless single term is used to express temperature along heated surface.

$$T_w = T_0 + C_m (X / a)^m q_m(0) \tag{26}$$

The regular pertubation method is the preferred analytical scheme for providing approximate solutions to the nonlinear ordinary differential equations whose principles have been thoroughly introduced in [20-21] . The flow and heat transfer series solution where ϵ is the small pertubation parameter, may be presented in the following form.

Taking power series of velocity and temperature fields yields

$$f = f_0 + \in f_1 + \in^2 f_2 + O(\in^3) \tag{27}$$

$$q_m = q_{m0} + \in q_{m1} + \in^2 q_{m2} + O(\in^3) \tag{28}$$

Substituting Eq. (27) into (20) and selecting at the various order yield

$$\in^0 : \frac{d^4 f_0}{d\eta^4} \tag{29}$$

$$\in^1: \frac{d^4 f_1}{d\eta^4} + \frac{A_1}{A_2}\left(\alpha\left(3\frac{d^2 f_0}{d\eta^2} + \eta\frac{d^3 f_0}{d\eta^3}\right)\right.$$
$$\left.-R\left(\frac{df_0}{d\eta}\frac{d^2 f_0}{d\eta^2} - \frac{d^3 f_0}{d\eta^3} f_0\right)\right) \quad (30)$$

$$\in^2: \frac{d^4 f_2}{d\eta^4} + \frac{A_1}{A_2}\left(\alpha\left(\frac{d^2 f_1}{d\eta^2} + \eta\frac{d^3 f_0}{d\eta^3}\right)\right.$$
$$\left.-R\left(\frac{df_0}{d\eta}\frac{d^2 f_1}{d\eta^2} + \frac{df_1}{d\eta}\frac{d^2 f_0}{d\eta^2} - \frac{d^3 f_0}{d\eta^3} f_1 - \frac{d^3 f_1}{d\eta^3} f_0\right)\right) \quad (31)$$

Substituting Eq. (28) into (23) and selecting at the various order yield

$$\in^0: \frac{d^2 q_{m0}}{d\eta^2} \quad (32)$$

$$\in^1: \frac{d^2 q_{m1}}{d\eta^2} + \frac{A_3}{A_4}\left(\Pr R\left(\frac{dq_{m0}}{d\eta} f_0 - m\frac{df_0}{d\eta} q_{m0}\right)\right.$$
$$\left.+\alpha \Pr\left(\eta\frac{dq_{m0}}{d\eta} + m q_{m0}\right)\right) \quad (33)$$

$$\in^2: \frac{d^2 q_{m2}}{d\eta^2} - \frac{A_3}{A_4}\left(\Pr R\left(\frac{dq_{m0}}{d\eta} f_1 + \frac{dq_{m1}}{d\eta} f_0\right.\right.$$
$$\left.\left.-m\frac{df_0}{d\eta} q_1 - m\frac{df_1}{d\eta} q_0\right) + \alpha \Pr\left(\eta\frac{dq_{m1}}{d\eta} + m q_{m1}\right)\right) \quad (34)$$

Leading order boundary condition is given as

$$f_0(0) = 0 \quad \frac{df_0}{d\eta}(0) = 0 \quad f_0(1) = 1 \quad \frac{df_0}{d\eta}(1) = 1 \quad (35)$$

Simplifying Eq. (29) applying the leading order boundary condition Eq. (35) yields

$$f_0 = -\eta^2(2\eta - 3) \quad (36)$$

Leading order boundary condition is given as

$$q_{m0}(0) = 1, q_{m0}(1) = 0 \quad (37)$$

Simplifying Eq. (32) applying the leading order boundary condition Eq. (37) yields

$$q_{m0} = 1 - \eta \quad (38)$$

First order boundary condition is given as

$$f_1(0) = 0 \quad \frac{df_1}{d\eta}(0) = 0 \quad f_1(1) = 1 \quad \frac{df_1}{d\eta}(1) = 1 \quad (39)$$

Simplifying Eq. (30) applying the first order boundary condition Eq. (39) yields

$$f_1 = \left(A_1\eta^2(\eta-1)^2(7\alpha + 32R + 56\alpha\eta + 10R\eta\right.$$
$$\left.-12R\eta - 12R\eta^2 + 8R\eta^3)\right)/\left(140A_2\right) \quad (40)$$

First order boundary condition is given as

$$q_{m1}(0) = 1, q_{m1}(1) = 0 \quad (41)$$

Simplifying Eq. (33) applying the first order boundary condition Eq. (41) yields

$$q_{m1} = \left(A_3 \Pr\eta(\eta-1)(10\alpha + 9R - 20\alpha m + 10\alpha\eta\right.$$
$$+18Rm + 9R\eta + 9R\eta^2 - 6R\eta^3 + 10\alpha m\eta + 18Rm\eta$$
$$\left.-42Rm\eta^2 + 18Rm\eta^3\right)/\left(60A_4\right) \quad (42)$$

The coefficient $\in^2$ for $F(\eta)$ and $q_m(\eta)$ in Eqs. (31) and (34) were too long to be mentioned here but it is expressed graphically in all the results and in the result validation, Table 2 and 3. Therefore final expressions for flow and heat transfer profile can be expressed as

$$f(\eta) = f_0(\eta) + f_1(\eta) + f_2(\eta) \quad (43)$$

$$q_m(\eta) = q_{m0}(\eta) + q_{m1}(\eta) + q_{m2}(\eta) \quad (44)$$

Table 2. Comparison of Values of H for Dimensionless Velocity Distribution. Where R=m=α=1and ϕ=0.0.

η	f(η)		
	NS	Present work	Error
0.0	0.0000	0.0000	0.0000
0.1	0.0308	0.0309	0.0001
0.2	0.1143	0.1143	0.0000
0.3	0.2355	0.2355	0.0000
0.4	0.3797	0.3797	0.0000
0.5	0.5322	0.5322	0.00000
0.6	0.6795	0.6795	0.00000
0.7	0.8093	0.8093	0.00000
0.8	0.9113	0.9113	0.00000
0.9	0.9770	0.9770	0.00000
1.0	1.0000	1.0000	0.00000

Table 3. Comparison of Values of H for Dimensionless Temperature Distribution. Where R=m=α=1and ϕ=0.0.

η	$q_m(\eta)$		
	NS	Present work	Error
0.0	1.000	1.0000	0.0000
0.1	0.8931	0.8932	0.0001
0.2	0.7858	0.7858	0.0000
0.3	0.6792	0.6792	0.0000
0.4	0.5742	0.5742	0.0000
0.5	0.4714	0.4714	0.0000
0.6	0.3711	0.3711	0.0000
0.7	0.2737	0.2737	0.0000
0.8	0.1793	0.1793	0.0000
0.9	0.0880	0.0880	0.0000
1.0	0.0000	0.0000	0.0000

3. Results and Discussion

The result generated through analytical solution for the nanofluid flow through the porous channel is reported graphically in Figs 2-11. It can be observed from Tables 2 and 3 that satisfactory agreement is established between the various methods of solution. The effect of various thermo-fluidic parameters on flow and heat transfer is reported graphically for the various numerical variation at constant parameters of R=5, m=α=2 and ϕ=0.05 unless otherwise stated. The Fig. 2 shows the effect of Reynolds parameter (R) on flow where it is demonstrated that quantitative increase in R causes a corresponding increase in velocity distribution which increases steadily from the stationery lower plate to the expanding/ contracting upper plate which can be physically explained as a result of increasing velocity boundary layer. Effect of expansion ratio (α) is depicted in Fig. 3 were it is shown from plot that increase in α leads to significant increase in velocity distribution which is as result of increasing injection variation which effect is prominent at the expanding/contracting plate.

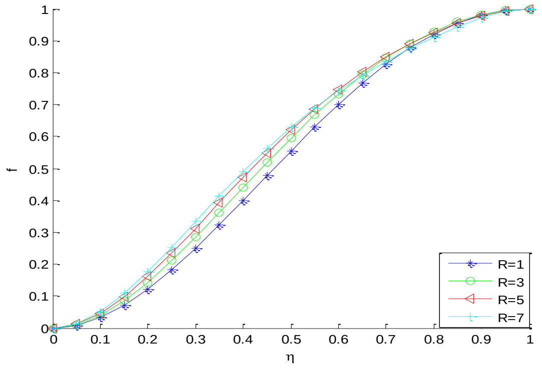

Figure 2. Effect of Reynolds number (R) on velocity profile.

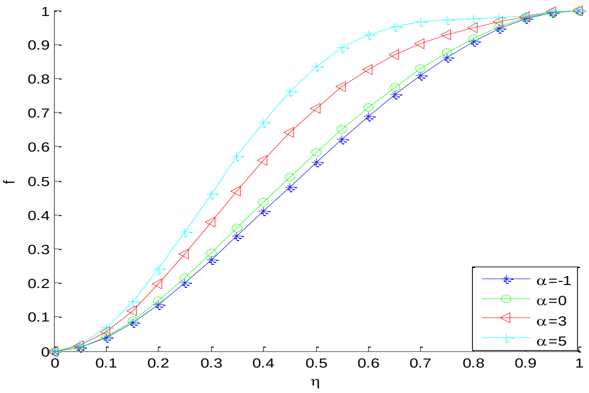

Figure 3. Effect of Expansion ratio (α) on velocity profile.

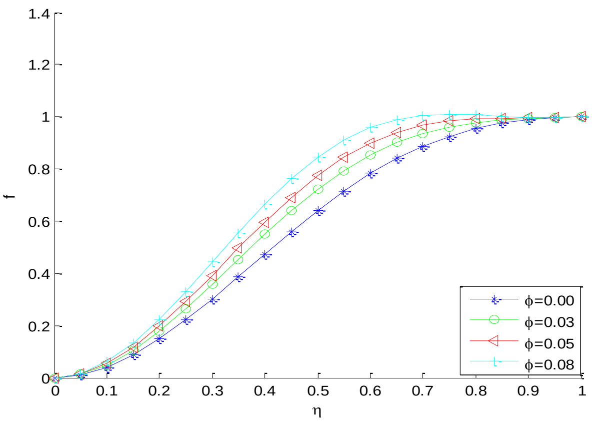

Figure 4. Effect of nanoparticle volume fraction (ϕ) on velocity profile.

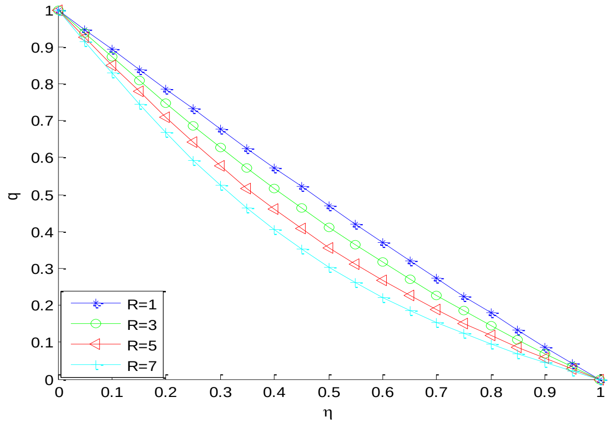

Figure 5. Effect of Reynolds number (R) on temperature profile.

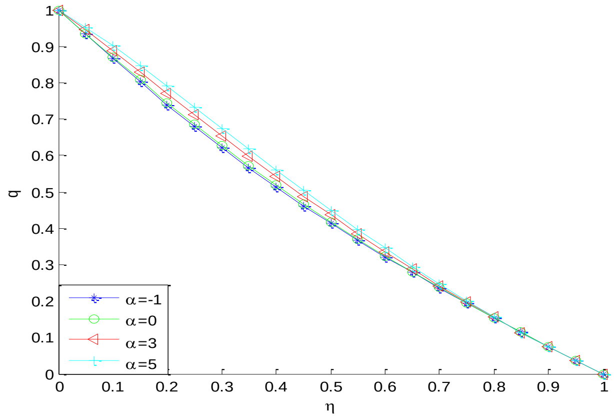

Figure 6. Effect of expansion ration (α) on temperature profile.

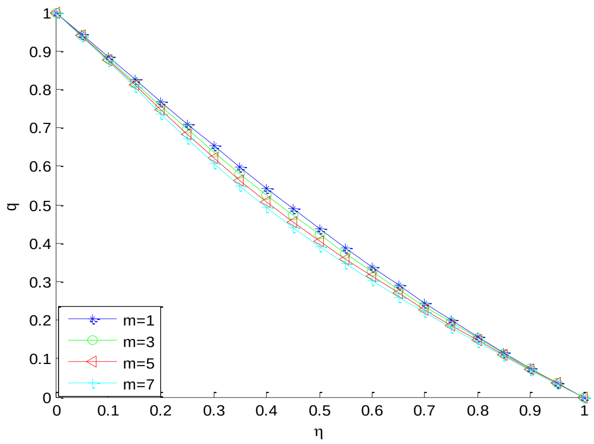

Figure 7. Effect of temperature power index (m) on temperature profile

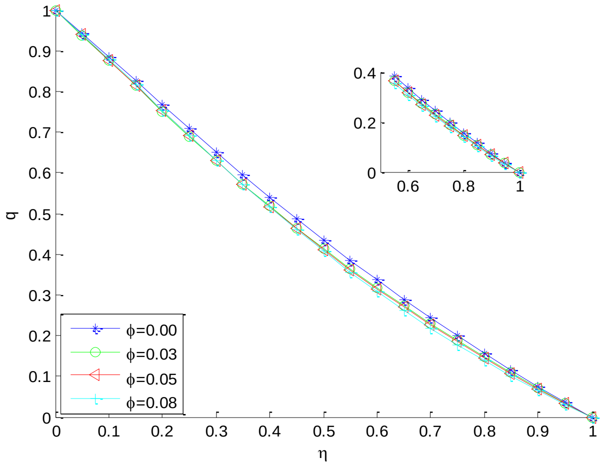

Figure 8. Effect of nanoparticle volume fraction (ϕ) on temperature profile

As nanoparticle volume fraction (ϕ) increases slight increase is observed in velocity profile due to increasing fluid thermal conductivity as illustrated in Fig. 4. Where the effect of fluid flow without nanoparticle is seen when ϕ=0, which present the lowest velocity profile this shows nanoparticle as significant effect on fluid flow. Reynolds parameter effect (R) on temperature distribution is seen in Fig. 5 which shows the significance of inertia effect against viscous effect were it can be depicted that increasing R leads to decrease in temperature distribution due to decreasing thermal boundary layer thickness which is maximum at the lower stationery plate and minimal at the upper plate. The Fig. 6 represent the expansion ratio (α) effect on temperature profile, which shows increase in temperature distribution as the quantitative values of α increases owing to the increase in injection velocity variations. Effect of temperature index (m) which allows single value of heat transfer across various points on heated surface to be obtained owing to polynomial wall temperature variation is presented in Fig. 7 which illustrates that increasing m shows a decreasing temperature profile. Nanoparticle fraction (ϕ) effect is observed from Fig. 8 which depicts increasing ϕ causes decrease in temperature distribution due to high heat and mass transfer caused by higher thermal conductivity which in turns causes a slight increase in thermal boundary layer.

4. Conclusion

Nanofluid flow and heat transfer through expanding or contracting porous channel is considered in this study where effect of thermo-fluidic parameters is examined on flow and heat transfer driven by injection. The regular perturbation analytical scheme is employed in solving the coupled system of higher order equations. Where obtained solutions were used to investigate parameter effects on fluid transport which is reported graphically for different cases of numerical variations. From results it is depicted that increasing Reynolds parameter causes increasing velocity distribution while increasing temperature power index demonstrates decreasing temperature effect. Study provides good advancement to applications such as fluid transport, power plant operations and manufacturing amongst others.

Conflict of Interest

The author declares there is no competing interest as regard publication of this paper.

Nomenclature

A	Wall permeability
A_{1-4}	Constant parameters in nanofluid
a	Distance between parallel plates
a(t)	Expand or contract function
C_p	Specific heat in constant pressure
C_{1-4}	Constants in trial function
F(η)	Stream function variable
K	Thermal conductivity
M	Temperature index
Nu	Nusselt number
p	Pressure
q	Heat transfer
R	Reynolds number
R(x)	Residual function
t	Time
T	Temperature
u	Velocity in x direction
v	Velocity in y direction
W(x)	Weighted function
x	Horizontal axes coordinate
y	Vertical axes coordinate

Greek symbols

α	Expansion ration
μ	Viscosity
ϕ	Nanoparticle volume fraction
ρ	Density
ψ	Stream function
η	Non-dimensional y direction $\left[y/a\right]$

Subscript

f	Fluid
nf	Nanofluid
s	Solid
w	Wall

References

[1] Pourmehran, O., Rahimi-Gorji, M., Hatami, M., Sahebi, S.A.R., Domairry, G., Numerical optimization of microchannel heat sink (MCHS) performance cooled by KKL based nanofluids in saturated porous medium, *Journal of the Taiwan Institute of Chemical Engineers*, Vol. 55, 49-68, 2015.

[2] Tang, W., Jing, D., Natural convection heat transfer in a nanofluid-filled cavity with double sinusoidal wavy walls of various phase deviations, I*nternational Journal of Heat and Mass Transfer*, Vol. 115, 430-440, 2017.

[3] Hatami, M., Sheikholeslami, M., Domairry, G., High accuracy analysis for motion of a spherical particle in plane Couette fluid flow by Multi-step Differential Transformation Method, *Powder Technology*, Vol. 260, 59-67, 2014.

[4] Hatami, M., Song, D., Jing, D.D., Optimization of a circular-wavy cavity filled by nanofluid under the natural convection heat transfer condition, *International Journal of Heat and Mass Transfer*, Vol. 98, 758-767, 2016.

[5] Ghasemi, S.E., Hatami, M., Mehdizadeh Ahangar, G.H.R., Ganji, D.D., Electro hydrodynamic flow analysis in a circular cylindrical conduit using least square method, *Journal of Electrostatics*, Vol. 72, 47-52, 2014.

[6] Ghasemi, S.E., Hatami, M., Sarokalaine, A.K., Ganji, D.D., Study on blood flow containing nanoparticles through porous arteries in presence of magnetic field using analytical methods, *Physica E: Low-dimensional System and Nanostructures*, Vol. 70, 146-156, 2015.

[7] Hatami, M., Ganji, D.D., Motion of a spherical particle on a rotating parabola using Lagrangian and high accuracy multi-step differential transformation method, *Powder Techonology*, Vol. 258, 94-98, 2014.

[8] Hatami, M. Jing, D., Optimization of a lid-driven T-shaped porous cavity to improve the nanofluids mixed convection heat transfer, *Journal of Molecular Liquids*, Vol. 231, 620-631, 2017.

[9] Kargar, A., Akbarzade, M., Analytical solution of Natural convection Flow of a non-Newtonian between two vertical parallel plates using the Homotopy Perturbation Method, *World Applied Sciences Journal*, Vol. 20, 1459-1465, 2012.

[10] Fakour, M., Vahabzadeh, A., Ganji, D.D., Hatami, M., Analytical study of micropolar fluid flow and heat transfer in a channel with permeable walls, *Journal of Molecular Liquids*, Vol. 204, 198-204, 2015.

[11] Hatami, M., Nanoparticles migration around the heated cylinder during the RSM optimization of a wavy-wall enclosure, *Advanced Powder Technology*, Vol. 28, 890-899, 2015.

[12] Choi, S.U.S, Engineering thermal conductivity of fluids with nanoparticles, Development and Application of Non-Newtonian Flows, *Argonne National Lab*, Vol. 66, 99-105, 1995.

[13] Farajpour, A., Rastgoo, A., Mohammadi, M., Vibration, buckling and smart control of microtubules using piezoelectric nanoshells under electric voltage in thermal environment, *Physica B: Condensed Matter*, Vol. 509, 2017.

[14] Wu, W., Massoudi, M., Yan, H., Heat Transfer and Flow of Nanofluids in a Y-Type Intersection Channel with Multiple Pulsations: A Numerical Study, *Energies*, Vol. 10, 2017.

[15] Sun, X., Yan, H., Massoudi, M., Chen, Z., Wu, W., Numerical Simulation of Nanofluid Suspensions in a Geothermal Heat Exchanger, *Energies*, Vol. 11, No 4 919, 2018.

[16] Hashimi, M.R., Hayat, T., Alsaedi, A., On the analytic solutions for squeezing flow of nanofluids between parallel disks, *Nonlinear Analysis Modeling and Control*, Vol. 17, No.4, 418-430, 2014.

[17] Khan, W. A., Aziz, A., Natural convective boundary layer flow over a vertical plate with uniform surface heat flux, *International Journal of Thermal Science*, Vol. 50, 1207-1217, 2011.

[18] Khan, W. A., Aziz, A., Double diffusive natural convection boundary layer flow in a porous medium saturated with a nanofluid over a vertical plate, prescribed surface heat, solute and nanofluid fluxes, *International Journal of Thermal Sciences*, Vol. 50, 2154-2160, 2011.

[19] Yao, S., Fang, T., Zhang, Y., Heat transfer of a generalized stretching/shrinking wall problem with convective boundary condition, *Communications in Nonlinear Science and Numerical Simulation*, Vol. 16, 752-760, 2011.

[20] Makinde, D., Aziz, A., Boundary layer flow of a nanofluid past a stretching sheet with convective boundary conditions, *International Journal of Thermal sciences*, Vol. 50, 1326-1332, 2011.

[21] Akinshilo, A.T., Olofinkua, J.O., Olaye, O., 2017, Flow and Heat Transfer Analysis of Sodium Alginate Conveying Copper Nanoparticles between Two Parallel Plates, *Journal of Applied and Computational Mechanics*, Vol. 3, 258-266, 2017.

[22] Sobamowo, M.G., Akinshilo, A.T., 2017, On the analysis of squeezing flow of nanofluid between two parallel plates under the influence of magnetic field, *Alexandria Engineering Journal*, 2017.

[23] Filobello-Niño, U., Vazquez-Leal, H., Boubaker, K., Khan, Y., Perez-Sesma, A., Sarmiento Reyes, A., Jimenez-Fernandez, V.M., Diaz-Sanchez, A., Herrera-May, A., Sanchez-Orea, J., Pereyra-Castro, K., 2013, Perturbation Method as a Powerful Tool to Solve Highly Nonlinear Problems: The Case of Gelfand’s Equation, *Asian Journal of Mathematics and Statistics*, 2013.

[24] Lim, C.W., Wu, B.S. A modified Mickens procedure for certain non-linear oscillators, *Journal of Sound and Vibration*, Vol. 257, 202-206, 2002.

[25] Cheung, Y.K., Chen, S.H., Lau, S.L., 1991, A modified Lindsteadt-Poincare method for certain strongly non-linear oscillators, *International Journal of Non-Linear Mechanics*, Vol. 26, 367-378, 1991.

[26] Fakour, M., Vahabzadeh, A., Ganji, D.D., Hatami, M., Analytical study of micropolar fluid flow and heat transfer in a channel with permeable walls, *Journal of Molecular Liquids*, Vol. 204, 198-204, 2015.

[27] Hatami, M., Nanoparticles migration around the heated cylinder during the RSM optimization of a wavy-wall enclosure, *Advanced Powder Techonology*, Vol. 28, 890-899, 2017.

[28] Tang, W., Jing, D., Natural convection heat transfer in a nanofluid-filled cavity with double sinusoidal wavy walls of various phase deviations, *International Journal of Heat and Mass Transfer*, Vol. 115, 430-440, 2017.

[29] Garoosi, F., Bagheri, G., Rashidi, M.M., Two phase simulation of natural convection and mixed convection of nanofluid in square cavity, *Powder Technology*, Vol. 275, 239-256, 2015.

[30] Garoosi, F., Rohani, B., Rashidi, M.M., Two phase modeling of mixed convection nanofluids in a square cavity with internal and external heating, *Powder Technology*, Vol. 275, 304-321, 2015.

[31] Garoosi, F., Jahanshaloo, L., Rashidi, M.M., Badakhsh, A., Alli, A., Numerical simulation of natural convection of the nanofluid in heat exchangers using a Buongiorno model, *Applied Mathematics and Computation*, Vol. 254, 183-203, 2015.

[32] Malvadi, A., Ganji, D.D., Brownian motion and thermophoretic effects of slip flow of alumina/water nanofluid inside a circular microchannel in the presence of magnetic field, *International Journal of Thermal Science*, Vol. 84, 196-206, 2014.

[33] Mehmood, A., Ali, A., Analytic solution of three dimensional viscous flow and heat transfer over a stretching surface by homotopy analysis method, *American Society of Mechanical Engineers*, Vol. 130, 21701-21707, 2008.